MULTI-DECADAL VARIABILITY OF ATLANTIC WATER HEAT TRANSPORTS AS SEEN IN THE COMMUNITY CLIMATE SYSTEMS MODEL VERSION 3.0

By

Kara Sterling

RECOMMENDED: _____

_____

_____

_____

Advisory Committee Chair

_____

Chair, Department of Atmospheric Sciences

APPROVED: _____

Dean, College of Natural Sciences and Mathematics

_____

Dean of the Graduate School

May 12, 2006

Date

MULTI-DECADAL VARIABILITY OF ATLANTIC WATER HEAT TRANSPORTS AS SEEN IN THE COMMUNITY CLIMATE SYSTEMS MODEL VERSION 3.0

A

THESIS

Presented to the Faculty

of the University of Alaska Fairbanks

in Partial Fulfillment of the Requirements

for the Degree of

MASTER OF SCIENCE

By

Kara Sterling, B.A., M.S.

Fairbanks, Alaska

May 2006

Abstract

Changes in oceanic heat transports from the North Atlantic to the Arctic, via Atlantic Water (AW), can have widespread impacts upon Arctic climate. Using a multi-century control simulation from the National Center for Atmospheric Research (NCAR) Community Climate Systems Model version 3.0 (CCSM3), the natural multi-decadal variability (MDV) of AW is characterized. Calculations of AW volume fluxes and heat transports into the Arctic are analyzed for the Svinøy transect, Fram Strait, and Barents Sea Opening (BSO), and compared with observations. Warm and cold phases of AW are examined through composite analysis, and quantified with respect to their effects on Arctic climate.

The model captures several key features of AW, such as the overall circulation and depth of the AW core, but over-estimates AW temperatures by about 1 °C. AW heat anomalies can be tracked from the Svinøy transect to the Arctic interior with a timescale of 13 years, which is comparable to observations. Composites reveal a deepening (shoaling) of the AW core during warm (cold) periods. Warm (cold) periods are also characterized by greater AW transports through the BSO (Fram Strait), implying the existence of an internal ocean feedback mechanism that helps to regulate oscillations of AW between warm/cold periods.

Table of Contents

Page

Signature Page.....i

Title Page.....ii

Abstract.....iii

Table of Contents.....iv

List of Figures.....v

List of Tables.....vi

I. Introduction.....1

II. Model and Data.....3

III. Results.....5

a. Atlantic Water (AW) Climatology in the CCSM3.....5

b. CCSM3 comparisons with observational AW entrance regions...7

i. Temperature versus Depth Profiles.....8

ii. CCSM3 and Observed Heat and Volume Fluxes.....10

c. CCSM3 Box Diagram Variable Means.....13

d. Multi-Decadal Variability (MDV) in the CCSM3.....15

i. Atlantic Water Core Temperature and Depth.....16

ii. Time Series for Box Diagram Variables.....17

e. Warm and Cold Composites in the CCSM3.....19

i. Composite Analysis.....20

ii. Ocean TEMP and Circulation.....22

iii. SLP, T_{ref}, and ICEFRAC.....25

IV. Summary and Conclusions.....27

V. Appendix A.....31

VI. Bibliography.....34

List of Figures

Page

Figure 1: Region of Study.....2
Figure 2a: Atlantic Water Core Temperature Climatology.....6
Figure 2b: Atlantic Water Core Depth Climatology.....6
Figure 3: Box Diagram for Ocean Transect Variables.....8
Figure 4a: TEMP @ Svinøy 63N, 3E.....9
Figure 4b: TEMP @ Fram 79.5N, 3-8.5E.....9
Figure 4c: TEMP @ BSO 71-79.5N, 31E.....9
Figure 4d: interior TEMP @ 85N, 120W.....9
Figure 5: CCSM3 versus Observational Data.....11
Figure 6: Box Diagram Variables.....14
Figure 7a: AWcoreDEPTH and AWcoreTEMP.....16
Figure 7b: TEMP at 60E.....16
Figure 8a: Svinøy and NwS Standardized TEMP.....18
Figure 8b: Fram, NwS, and BSO Standardized TEMP.....18
Figure 8c: Eurasian Basin and BSO Standardized TEMP.....18
Figure 8d: Eurasian Standardized TEMP, ICEVOL, & ICEFRAC.....18
Figure 9: Warm and Cold Composites for the Box Diagram Variables 21
Figure 10a: Warm TEMP Anomalies.....23
Figure 10b: Cold TEMP Anomalies.....23
Figure 11a: MEAN, WARM - MEAN, and COLD - MEAN for TREFHGT [°C]...26
Figure 11b: MEAN, WARM - MEAN, and COLD - MEAN for PSL [mb].....26
Figure 11c: MEAN, WARM - MEAN, and COLD - MEAN for ICEFRAC [%].....26

List of Tables

Page

Table 1: Warm and Cold Composites.....20

I. Introduction

Recent documented changes in Arctic climate bring cause for concern about the effects of greenhouse warming on our environment (ACIA 2005, Dickson 1999). Along with warmer Arctic air temperatures and decreased in sea ice extent and thickness, (Rothrock et al. 1999, Serreze et al. 2000, Schauer et al. 2004), ocean temperatures in the North Atlantic have also increased (Carmack et al. 1998, Polyakov et al. 2004, Orvik and Skagseth 2005). Changes in oceanic heat transports from the North Atlantic to the Arctic can have widespread impacts on the local climate (Mork & Blindheim 2000, Rhines & Hakkinen 2003), and could even bring about changes in the global Thermohaline Circulation (THC) (Rahmstorf 1999, Hansen et al. 2004). Hence, detecting fluctuations in these heat transports from the North Atlantic is of great interest when observing changes in Arctic climate.

The North Atlantic is the main conduit for oceanic heat transports into the Arctic, for which the dominant heat source is the warm and saline waters brought from the Gulf Stream north, by the North Atlantic Current (NAC). Continuing poleward from the NAC, the Norwegian Atlantic Current (NwAC) transports the warm Atlantic Water (AW) into the Norwegian Sea (NwS) before branching into a western and eastern NwAC (Figure 1).

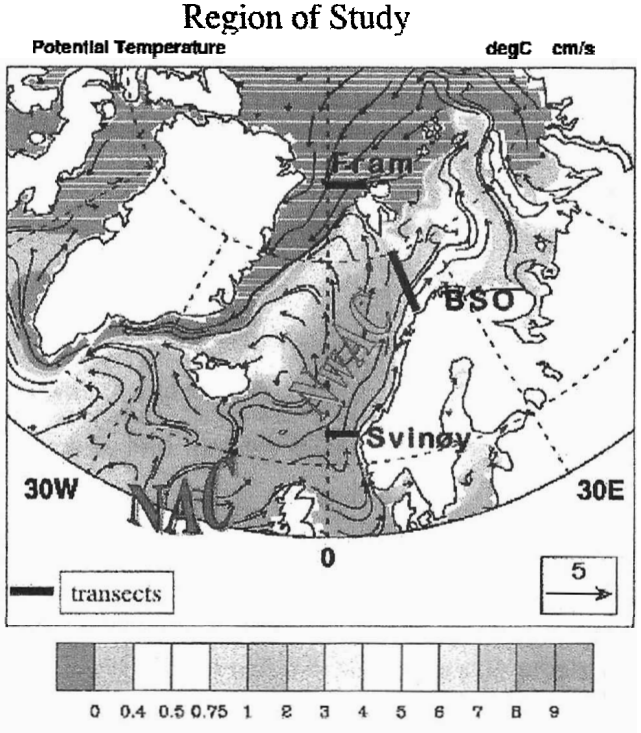

Figure 1. CCSM3 SST [°C] and surface current vectors [reference vector of 5 cm/s] for the North Atlantic, showing the North Atlantic Current (NAC), the Norwegian Atlantic Current (NwAC), and Atlantic Water inflow transects for the Svinøy section, the Fram Strait, and the Barents Sea Opening (BSO).

The western branch feeds AW into the Arctic through the Fram Strait, while the eastern branch of AW enters the Arctic through the Barents Sea Opening (BSO).

En route to the Arctic, the saline AW cools and becomes denser, subsiding below the surrounding waters of the Nordic Seas (Greenland, Iceland, and Norwegian Seas, or GIN Seas). This results in a warm, sub-surface AW layer occupying depths of 150-500 m beneath the Arctic Ocean surface. This AW layer is the key pathway by which variability from the North Atlantic is transferred into the Arctic. Characterized by temperatures greater than 0 °C, AW is also the dominant source for heat in the Arctic Ocean. Thus, changes in AW can have large impacts on Arctic climate.

To assess the characteristics of AW transports into the Arctic, calculations of volume flux and heat transport are calculated based upon the observational data. While past estimates had to rely upon the sparsely sampled measurements of AW (Simonsen and

Haugen 1996), currently, data describing AW is being collected at several mooring transects throughout the North Atlantic (Furevik 2001, Schauer et al. 2004, Orvik and Skagseth 2005).

This data from observational mooring transects has helped to characterize variability of AW over the past decade, but it does not provide information concerning the multi-decadal variability (MDV) of AW. In a collection of observational data by Polyakov et al. (2004), a 100-year data set for the Arctic Ocean was compiled and used to examine the MDV of AW. It was found that AW oscillated between a high and a low phase at time scales of 50-80 years, and that the MDV of AW was closely connected to Arctic MDV found in surface air temperature, sea level pressure, sea ice, and salinity (Polyakov et al. 2004).

In light of recent warming trends in the Arctic, it would be ideal to separate the extent to which changes in AW are due to natural MDV, versus greenhouse warming. To this end, a multi-century control simulation (1990s CO_2 level) of the global climate model Community Climate Systems Model version 3.0 (CCSM3) is used to assess the natural MDV of AW. Supplying full coverage of dynamically consistent variables for the Arctic, the CCSM3 permits the investigation of possible mechanisms governing changes in AW heat transports. In addition, the model provides more realizations of multi-decadal oscillations than available from observational data, allowing a more complete characterization of AW variability. Thus, focus of this thesis, is concentrated on the MDV of AW seen through oceanic heat and volume transports into the Arctic. Warm and cold phases of AW are examined through composite analysis and quantified with respect to their effects on Arctic climate.

II. Model and Data

The National Center for Atmospheric Research (NCAR) Community Climate Systems Model version 3.0 (CCSM3) consists of four components models that represent the atmosphere, ocean, cryosphere, and land surface. These component models are linked

through a flux coupler where no corrections are applied to the fluxes. There have been major improvements from previous versions of the model in the parameterizations of cloud processes, aerosol radiative forcing, land-atmosphere fluxes, and sea-ice dynamics (Collins et al, 2005). The CCSM3 system components consist of the; atmosphere, CAM version 3.0 (Collins et al. 2004, 2005b), land surface, CLM version 3.0 (Oleson et al. 2004, Dickinson et al. 2005), sea ice, CSIM version 5.0 (Briegleb et al. 2004), and ocean, which is based upon POP version 1.4.3 (Smith and Gent 2002).

The Community Atmosphere Model (CAM3, Collins et al. 2005b), is a global atmospheric general circulation model, with 26 vertical levels and is based upon the Eulerian spectral dynamical core with triangular truncation at 31, 42, and 85 wave numbers, horizontal resolutions of approximately 3.75°, 2.8° and 1.4°, respectively (Collins et al. 2004, 2005b). The Community Land Model (CLM, Oleson et al. 2004, Dickinson et al. 2005) grid is identical to that of CAM3.

The ocean general circulation model is an extension of the Parallel Ocean Program (POP, Danabasoglu et al. 2005) originally developed at Los Alamos National Laboratory. POP has 40 vertical levels and a nominal horizontal resolution of 1°: uniform zonal resolution of 1.125° and meridional resolution that varies from 0.27° near the equator to more than 0.5° poleward of 30°. The Community Sea-Ice Model (CSIM, Briegleb et al. 2004) shares the same grid as the ocean model. To simplify the analysis and comparisons between oceanic and atmospheric variables, all ocean data was remapped[1] from the POP grid onto the atmospheric T42 grid.

A 1000-year T42 (2.8° latitude x 2.8° longitude) control simulation of CCSM3 (b30.004) is based on 1990 greenhouse gas concentrations and provides key climate parameters for examining the variability of Atlantic Water (AW) in the context of Arctic

[1] The translation coefficients used to interpolate from the POP to the T42 grid, apply to the surface topography only, implying that remapped levels below the surface may be erroneous near boundaries due to the surface topography not necessarily being applicable with depth. However, comparisons between the ocean POP data and the remapped (T42) ocean data, exhibit no problematic differences.

climate. Since the multi-decadal time scale is of interest, annually averaged model data is analyzed for 650 years (specifically years 350 to 999) of the control integration. Variables that are examined include ocean Potential Temperature (TEMP) and zonal (U) and meridional (V) current vectors, along with atmospheric Sea Level Pressure (SLP), Surface Heat Flux (SHF), 2-meter Reference Height Temperatures (REFHT, T_{ref}), ice fraction (ICEFRAC), and ice volume (ICEVOL).

III. Results

The model over-estimates AW temperatures by about 1 °C, but captures realistic AW circulation, depth, and transports (sections a, b & c). The AW core was found to deepen (shoal) during warm (cold) composites, and AW heat anomalies can be tracked from the Svinøy transect to the Arctic interior with a timescale of 13 years (section d). Warm (cold) periods are also characterized by greater AW transports through the BSO (Fram Strait), implying the existence of an internal ocean feedback mechanism that helps to regulate oscillations of AW between warm/cold periods (section e).

a. Atlantic Water (AW) Climatology in the CCSM3

Resulting from the subduction of warm, saline, North Atlantic water as it flows into the Arctic Ocean; subsurface Atlantic Waters (AW) are characterized by ocean potential temperatures greater than 0 °C. To construct the AW layer, the maximum ocean TEMP value, and the depth, z(t), at which it occurs, were extracted from the vertical temperature profile at each grid point for the Arctic Ocean (70-90°N, 0-360° longitude). This resulted in a layer defined as the AW core temperature (AWcoreTEMP), [°C], as well as an AW core depth (AWcoreDEPTH), [m]. Figure 2 displays the climatological mean for the

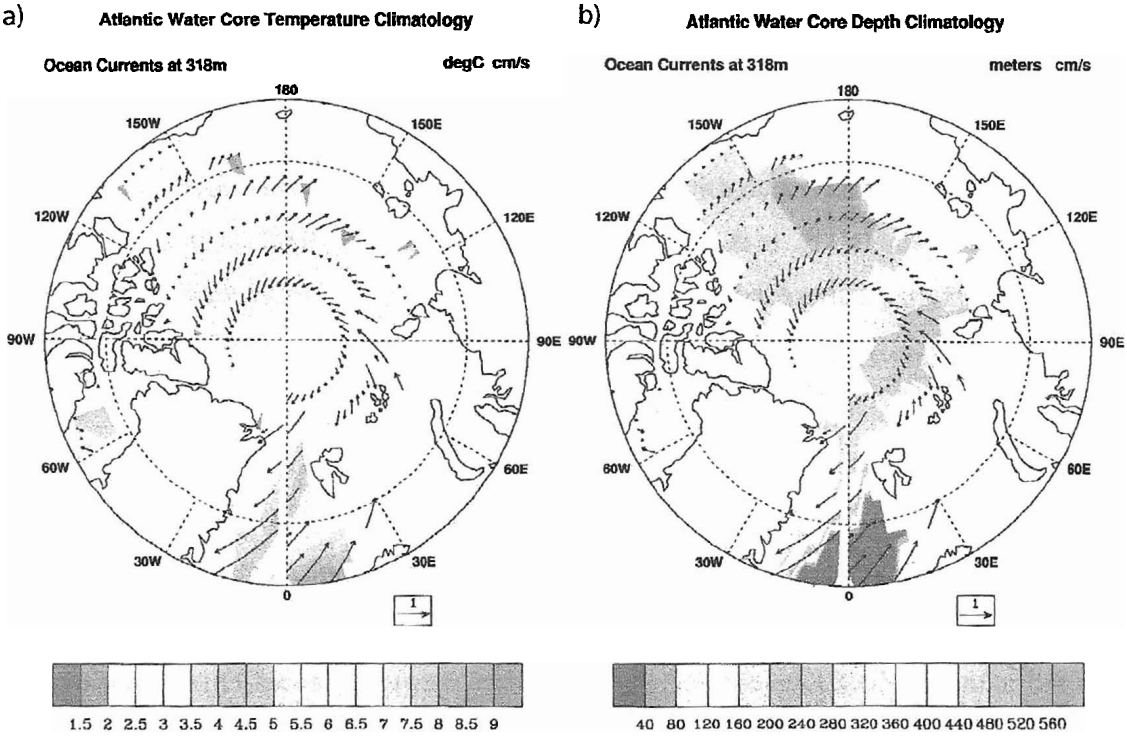

Figure 2. a) Core Atlantic Water temperatures [°C], and b) depths [meters]; both overlaid with 318m level currents [1 cm/s reference vector].

AWcoreTEMP and AWcoreDEPTH, with model temperatures of the AW core ranging from 2 °C in the Eurasian Basin to 3 °C moving into the Canadian Basin. The AW layer temperature ranges from approximately 2 °C in the eastern arctic to 0.4 °C in the western Arctic Basin (Polyakov et al 2004). A comparison with the CCSM3 climatology suggests that the model overestimates AW temperatures by 1-1.5 °C. The depth range of the AWcoreTEMP compares favorably with observations with typical values between 150-500 [m] (Polyakov et al. 2004). However, model depth temperature profiles taken from the Arctic interior show no clearly defined lower boundary of the AW layer, with profile temperatures decreasing steadily with increasing depth, z (t), but never cooling past 1.5 °C (see Figure 4d).

Based on the climatological AWcoreDEPTHs (Figure 2b), the 381 m level was determined to be representative of the AW layer circulation. The annually averaged 381m current vectors (U, V) were then extracted and overlaid onto the AWcoreTEMP

and AWcoreDEPTH climatologies (Figures 2a, b). The subsurface flow largely reflects the surface circulation, with inflow of AW into the Arctic occurring through two main passageways: 1) the Fram Strait, and 2) the Norwegian, Barents, and Kara Seas. The simulated CCSM3 AW is verified upon comparison with observed pathways of AW inflow (Orvik et al. 2001, Polyakov et al. 2004, Schauer et al. 2004), and found to be accurate. The anticyclonic gyre located at the surface of the Arctic Basin and displayed by CCSM3, is also in agreement observations. In nature, with increasing ocean depth, this gyre switches direction and becomes cyclonic in accordance with geostrophic flow (Polyakov et al. 2004). The climatological CCSM3 circulation in the AW core is anticyclonic. Moving from the AW core, the gyre circulation becomes weak and disoriented with increasing depth, but never[2] becomes cyclonic. However, since only the long-term mean is considered here, it is possible that the circulation is cyclonic during certain periods in time that were not examined here. While the CCSM3's inner basin circulation is largely capable of displaying realistic AW flow, modeled Arctic Ocean boundary currents are weaker than observed. Weak boundary currents seen in the CCSM3 could be a problem for analyzing realistic volume transports of AW into the Arctic from the Barents and Kara Seas. The model circulation displayed by the U, V, current vectors also appears to underestimate the observed strength of AW inflow through the Fram Strait, a point that will be discussed further in section b. ii.

b. CCSM3 comparisons with observational AW entrance regions

To evaluate the model circulation, flow from the CCSM3 is compared with flow measurements taken from sections where observations of AW are available. Observational mooring transects that monitor AW inflows are used to examine the CCSM3 AW simulation. Specifically, the CCSM3 output is compared with observed volume fluxes, heat transports, and TEMPs taken from the: 1) Svinøy transect, (Orvik and Skagseth 2005, Orvik et al. 2001, Mork and Blindheim 2000), 2) the Fram Strait

[2] Ocean TEMP data was analyzed from the surface down to 2375m.

(Schauer et al. 2004, Simonsen and Haugan 1996), and 3) the Barents Sea Opening (BSO) (Ingvaldsen 2004, Simonsen and Haugan 1996, Blindheim 1989). Together, these three observational transects cover the major pathways of AW inflow into the Arctic Ocean. Similar transects are constructed from the CCSM3 data and are used in conjunction with the observational data to verify AW inflow and examine variability in heat transports to the Arctic Ocean. The CCSM3 regions of study chosen for validation against observational mooring transects include; the Svinøy Transect [63°N, 3°E], Fram Strait [79.5°N, 3-8.5°E], and BSO [71-79.5°N, 31°E], a box diagram for which is shown in Figure 3. Variables of interest for the AW inflow transects include: volume flux, heat

Box Diagram for Ocean Transect Variables

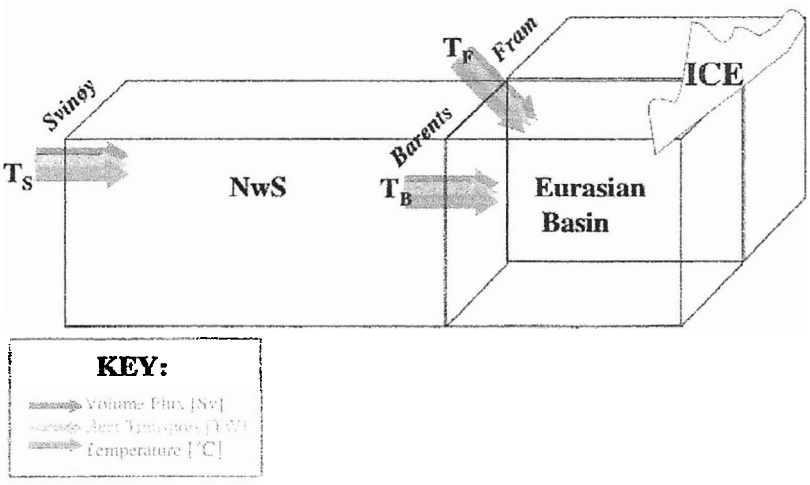

Figure 3. The CCSM3 region of study and transects (see Figure 1), shown as a box diagram with the variables of interest defined in the key.

transport, and temperature (see Appendix A).

i. Temperature versus Depth Profiles

Since the goal is to compare volume fluxes and heat transports with the observational data, spatially similar CCSM3 transects were chosen and the climatological cross-sectionally averaged temperature versus depth profiles compared (Figure 4).

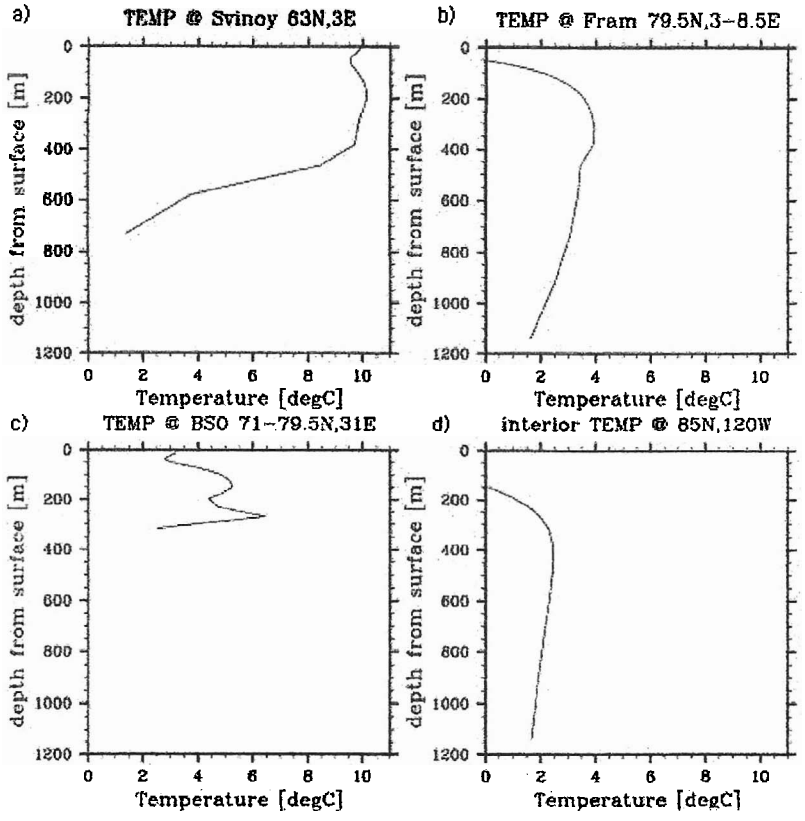

Figure 4. CCSM3 temperature [°C], profiles for the a) Svinøy, b) Fram, and c) BSO transects, and d) the interior Arctic Basin.

Specifically, the CCSM3 depth level, z(t), for the lower boundary of the AW layer, and the vertically averaged temperature, are compared with the mooring measurements. For the Svinøy transect, using Figure 4a, the CCSM3 AW lower boundary is taken to be at 600 m. This would put the CCSM3 AW temperature cutoff in the Svinøy transect to be T > 4 °C, which compares favorably with the observational AW transport calculations which use the 5 °C isotherm for the lower boundary (Orvik et al. 2001, Orvik and Skagseth 2005). In the Fram Strait (Figure 4b), the CCSM3 AW inflow cutoff depth is taken to be at 1000 m. This compares well with Schauer et. al. 2004 transport calculations, which use a lower boundary of 1000 m and a AW temperature cutoff of T > 1 °C. For the BSO, both in the CCSM3 and observations, the entire depth of the water column is considered AW inflow (Figure 4c) (Ingvaldsen 2004, Simonsen and Haugan

1996). The vertically averaged temperature in the CCSM3 transects is warmer than observations in the Svinøy transect, but cooler than observations from the Fram and BSO (see Figure 5, red). However, the temperature versus depth profiles taken over the AW inflow transects reveal similar boundaries and temperature characteristics of the AW layer in both the observations and the CCSM3. This implies that, even with the models slightly erroneous temperatures, the CCSM3 can be used to examine and compare oceanic volume and heat transports of AW into the Arctic.

ii. CCSM3 and Observed Heat and Volume Fluxes

For the Svinøy, Fram, and BSO inflows, the volume flux and heat transport were calculated according to the method outlined in Appendix A. Their long-term means and standard deviations were then used for comparisons with the observational mooring records. Shown along with vertically averaged AW inflow temperatures (red), is the climatological volume flux (blue), and heat transport (orange), (Figure 5). For each

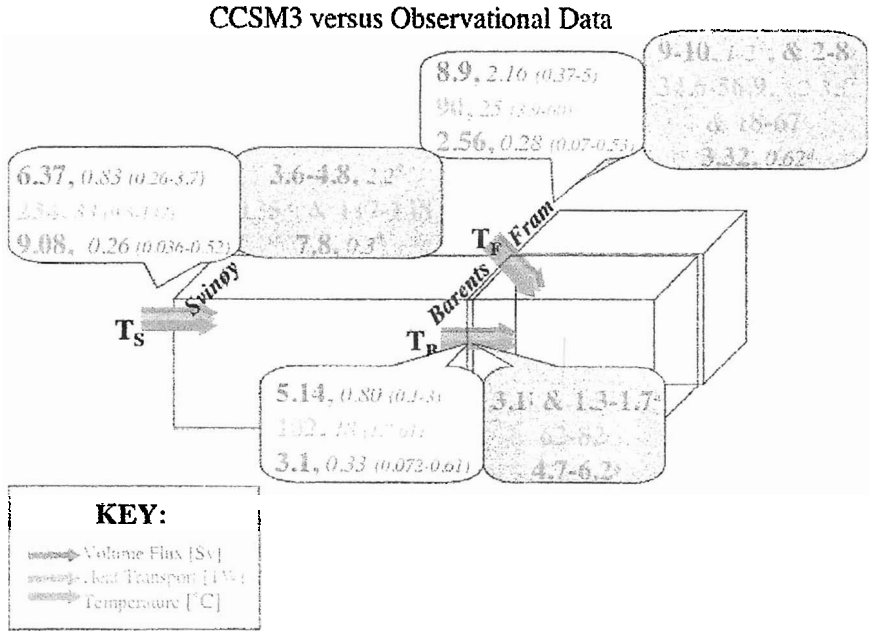

Figure 5. Volume Flux [Sv], Heat Transport [TW], and Temperature [°C], means, standard deviations, σ's, and a range of 5-year running standard deviations, σ_{5yr}'s, for the Svinoy, Fram and BSO transects. Symbols denote the following observational papers: *(Orvik and Skagseth 2005), ^ (Mork and Blindheim 2000), † (Schauer et al. 2004), § (Simonsen and Haugen, 1996), ‡ (Schauer et al. 2004; data), ¡ (Blindheim, 1989), and ª (Ingvaldsen, 2004).

quantity there is a sequence of numbers; the first number is the long-term mean, the second number is the standard deviation (σ) based upon the entire 650-year time series, and the third number, seen in parenthesis, gives the range of 5-year running σ's, or σ_{5yr}'s. Since most mooring data is only 5 to10 years in length, the range of 5-year running σ's indicates what may be expected if the model record was of similar length to the observations.

For the Svinøy transect, the CCSM3 produced a volume flux of 6.37 Sv, with σ_{5yr}'s in the range of 0.26-3.7; a heat transport of 234 TW with σ_{5yr}'s in the range of 9.5-137; and an inflow temperature of 9.08 °C, with σ_{5yr}'s in the range of 0.036-0.52. Observational measurements given in Orvik and Skagseth (2005), show Svinøy volume fluxes in the range of 3.6-4.8 Sv with a σ of 2.2, heat transports from 117-148 TW, and a temperature of 7.8 °C with a σ of 0.3. Also, Blindheim 1990, estimated a volume flux of 2.9-7.9 Sv, and Mork and Blindheim 2000, gave a Svinøy heat transport calculation of 135 TW. In

the Svinøy transect, as mentioned before, the model overestimates the observed temperature by about 1 °C. The CCSM3 also overestimates the observed volume flux by about 2 Sv based upon data by Orvik and Skagseth 2005, but is within the range of possibilities (1.4 - 7.0 Sv) using their observational standard deviation. The CCSM3 volume flux for the Svinøy transect is also within the range of those given by Blindheim 1990. Due to the combined over-estimations in temperature and volume flux, CCSM3 heat transport calculations are also larger than those found in observations.

In the Fram Strait, the CCSM3 long-term mean volume flux is 8.9 Sv with σ_{5yr}'s from 0.37-5. There is a heat transport of 90 TW with σ_{5yr}'s in the range of 3.9-60, and a temperature of 2.56 °C with σ_{5yr}'s from 0.07-0.53. Observational Fram Strait volume flux measurements by Schauer et al. 2004 gave 9-10 Sv with a σ_{5yr}'s of 1-2, and estimates by Simonsen and Haugan 1996, suggested a volume flux between 2-8 Sv. Hence, the CCSM3 volume flux for the Fram compares favorably with observational mooring data, possibly with the CCSM3 slightly under-estimating the flow. From the 1997-2004 observational mooring data used in Schauer et al. 2004, the average AW inflow temperature observed at 250 m depth through the Fram was found to be 3.3 °C. This would suggest that the CCSM3 temperature in the Fram is cooler than that observed. However, the CCSM3 temperature was vertically averaged over an AW layer extending down to1000 m depth in the Fram, implying that the accuracy of CCSM3 temperatures may be more complicated than this simple comparison suggests (recall Figure 3b). Heat transport observations for the Fram range from 34.6 to 56.9 TW, with a standard deviation of 3.2-3.3 (Schauer 2004), and were also estimated as somewhere between 18-67 TW (Simonsen and Haugan 1996). The CCSM3 over-estimates heat transport through the Fram by 25-50 TW.

Through the BSO, the modeled volume flux was 5.14 Sv with σ_{5yr}'s from 0.1-3, the heat transport was 102 TW with σ_{5yr}'s of 1.7-61, and the temperature was 3.1 °C with σ_{5yr}'s from 0.072-0.61. From the observations, volume fluxes for the BSO measured 3.1 Sv, (Blindheim 1989), and 1.3-1.7 Sv (Ingvaldsen 2004). Heat flux and temperature

measurements estimated from Simonsen and Haugan 1996, range from 62 to 82 TW and 4.7 to 6.2 °C. The CCSM3 overestimates the volume flux by about 2 Sv, however, the temperature is 1-2 °C lower than observations, which results in only a slightly increased modeled heat transport for the BSO. The larger estimate for volume flux seen in the CCSM3 is likely the result of slightly different transect locations and extents between the modeled data and mooring data. Again, the colder temperatures seen in the CCSM3 are probably a result of averaging over the entire vertical temperature profile.

While the model overestimates the temperature in the Svinøy transect, it underestimates ocean temperatures farther poleward in the Fram Strait and in the BSO. In general, the model circulation is stronger and the volume fluxes are larger than the observed, with the exception that modeled transport of AW in the Fram Strait is reasonable to weak. However, in recent observations by Schauer et al. 2004, a main outcome of the paper was how the observational mooring program produced higher than expected volume fluxes of AW into the Arctic through the Fram Strait. The CCSM3 also reproduces variability well within the range seen in the observations of AW volume flux, heat transport, and temperature.

c. CCSM3 Box Diagram Variable Means

Continuing to budget the heat coming into the Arctic, further CCSM3 variables for AW inflow were analyzed; these included SHF, ocean basin temperature, ice fraction and ice volume[3]. Figure 6 shows alongside the AW inflow transects; the long-term means and

[3] The ice fraction time series provides more information on variability differences between sea ice in the Eurasian Basin versus the Canadian Basin, it is also more readily comparable with observational data. Ice volume, however, is more useful when trying to calculate the effects of AW heat transport variability on Arctic sea ice.

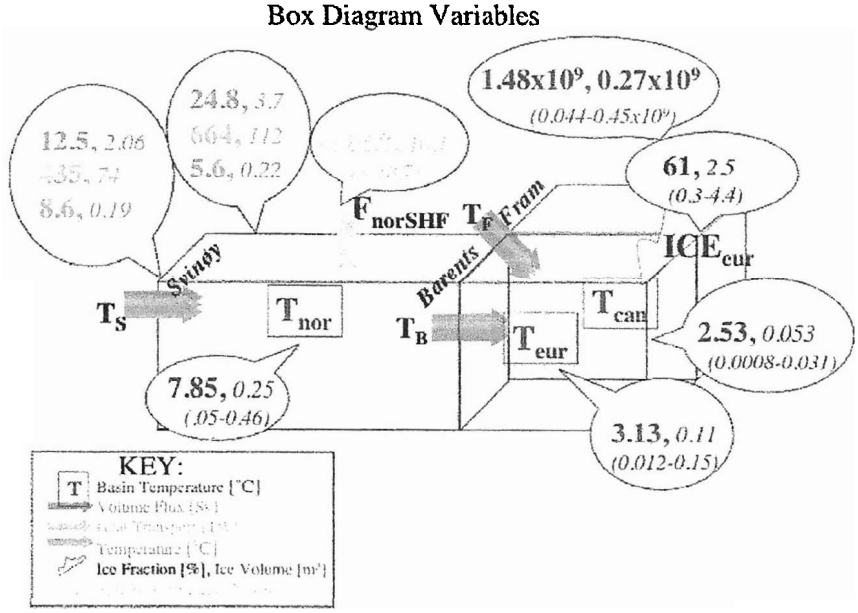

Figure 6. Diagnoses of the CCSM3 also included means and σ's for the (from the upper L, clockwise): extended Svinoy section, western boundary of the Norwegian Sea, the Norwegian Sea SHF and basin temperature, the Eurasian and Canadian basin temperatures, and the Eurasian Basin ice volume and ice fraction.

standard deviations for the Norwegian Sea SHF, the Norwegian Sea, Eurasian, and Canadian Basin temperatures, the Norwegian Sea western boundary inflow transports, the extended Svinøy transect, and the Eurasian Basin ice fraction and ice volume. Looking at Figure 6, the progression of AW through the Svinøy, Fram, and BSO transects can also be tracked by following ocean basin temperatures.

Looking first at the Norwegian Sea and using a representative depth for the AW layer, the basin temperature was averaged from the surface to the 150 m layer and found to be 7.85 °C. The extracted AW core shown in Figure 2a, was then split into two regions using the 30°W or 150°E longitude line, and area averaged from 80-90°N. This resulted in a Eurasian Basin temperature and a Canadian Basin temperature. For the Eurasian Basin the AWcoreTEMP is 3.1 °C, and the Canadian basin shows an AWcoreTEMP of 2.5 °C.

For the region of the Norwegian Sea[4], the atmosphere to ocean Surface Heat Flux (SHF) is calculated along with AW inflow transports for the western boundary. The Norwegian Sea SHF was found to be –114.8 W/m^2, where a negative flux is heat going out of the ocean, or cooling. The western boundary gave an AW inflow volume flux of 3.7 Sv, with a heat transport of 100 TW and an inflow temperature of 5.6 °C. The CCSM3 extended Svinøy transect was taken over [63°N, 3-8.5°E]. The extension of the Svinøy transect and the inclusion of a western boundary for the Norwegian Sea were done to further observed specific circulation changes possibly related to the warm and cold periods (see sections e. i, ii.) For the extended Svinøy transect, the CCSM3 had a volume flux of 12.5 Sv, a heat transport of 438TW, and an inflow temperature of 8.6 °C. The Eurasian Basin sea ice data is also examined, with an area averaging north of 70N resulting in a ice fractional mean of 61%, and a total ICEVOL of 1.48e09 m^3. For each variable shown in Figures 4 and 5, time series from the CCSM3 simulation were also examined and are discussed in section d. ii.

d. Multi-Decadal Variability (MDV) in the CCSM3

To examine the multi-decadal variability (MDV) of AW displayed by the CCSM3, the 650 years of AWcoreTEMPs and AWcoreDEPTHs were standardized by location and then area averaged over 80-90°N (Figure 7a).

[4] [65.5-71°N, 0-20°E]

a) AWcoreDEPTH and AWcoreTEMP

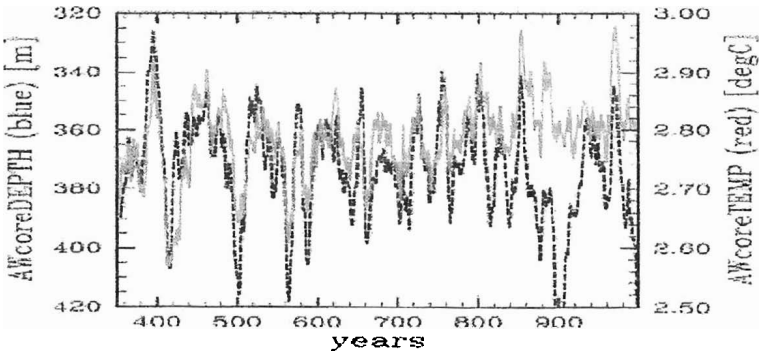

b) TEMP at 60°E

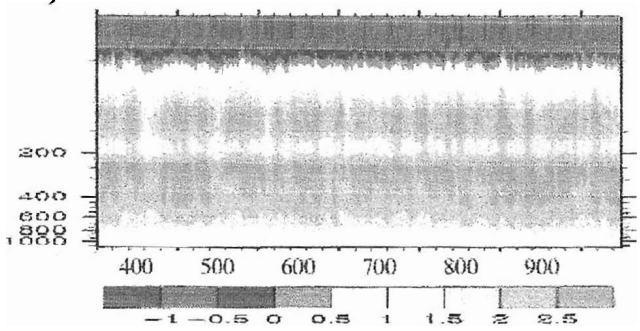

Figure 7. a) Area averaged from 80-90°N, standard deviations for core Atlantic Water temperatures (red) [°C] and depths (black) [m], for years 350-999. b) Hovmöler for an ocean slice averaged over [70-90°N, 60°E], showing temperature [°C] with depth [m] for years 350-999.

i. Atlantic Water Core Temperature and Depth

The modeled AW core displays MDV with period lengths between 30-70 years, and shows an inverse correlation between AWcoreTEMPs and AWcoreDEPTHs (note the inverted AWcoreDEPTH y axis on Figure 7a). The two time series correlate at –0.46, which is significant at 99% using the Wilcoxon signed-rank test. This implies that warm (cold) AWcoreTEMPs occur along with shallow (deep) AWcoreDEPTHs, a process that has also been noted in observations (Polyakov et al. 2004). It is interesting to note that starting around year 850, something occurred which causes a separation between the anomalies of the two variables until approximately year 930. A correlation of the two time series over years 350-850 yields –0.665.

A probable mechanism for this correlation originates from the idea that anomalously warm AWcoreTEMPs are associated with increased flow into the Arctic, occurring from

enhanced southwesterly atmospheric circulations over the North Atlantic subduction zone. These southwesterly circulations are often part of a larger cyclonic system, such as the positive NAO/AO or a strong localized system. Strong cyclonic circulation over the Arctic Ocean would induce a divergence at the ocean surface, causing an upwelling of the AW layer (Polyakov et al. 2004). A hovmöler (Figure 7b) showing an ocean slice for 60°E averaged over [70-90°N], for year's 350-999, shows an increase (reduction) in the thickness of the AW core occurring during periods where the temperature is warmer (cooler). Consistent with the proposed mechanism above, this also agrees with an increase in AW inflow making the AW core have more volume.

ii. Time series for Box Diagram Variables

The above mechanism implies a relationship between AW inflow temperatures, atmospheric circulation over the AW subduction zone, and AW MDV. To begin reviewing this relationship, time series of the CCSM3 variables depicted in Figures 5 & 6 are examined. A correlation analysis between climate variable time series was performed in order to determine the coherence between the series and to estimate the time taken for heat anomalies to propagate from the Svinøy transect to the Arctic interior.

At each of the three AW inflow transects (Figure 5), the time series for volume flux, heat transport, and temperature are significantly correlated at greater than 95%. Hence, the AW inflow temperature time series at the three transects is chosen to use for comparisons with other climate variables. While the time series shown in Figure 8 have a

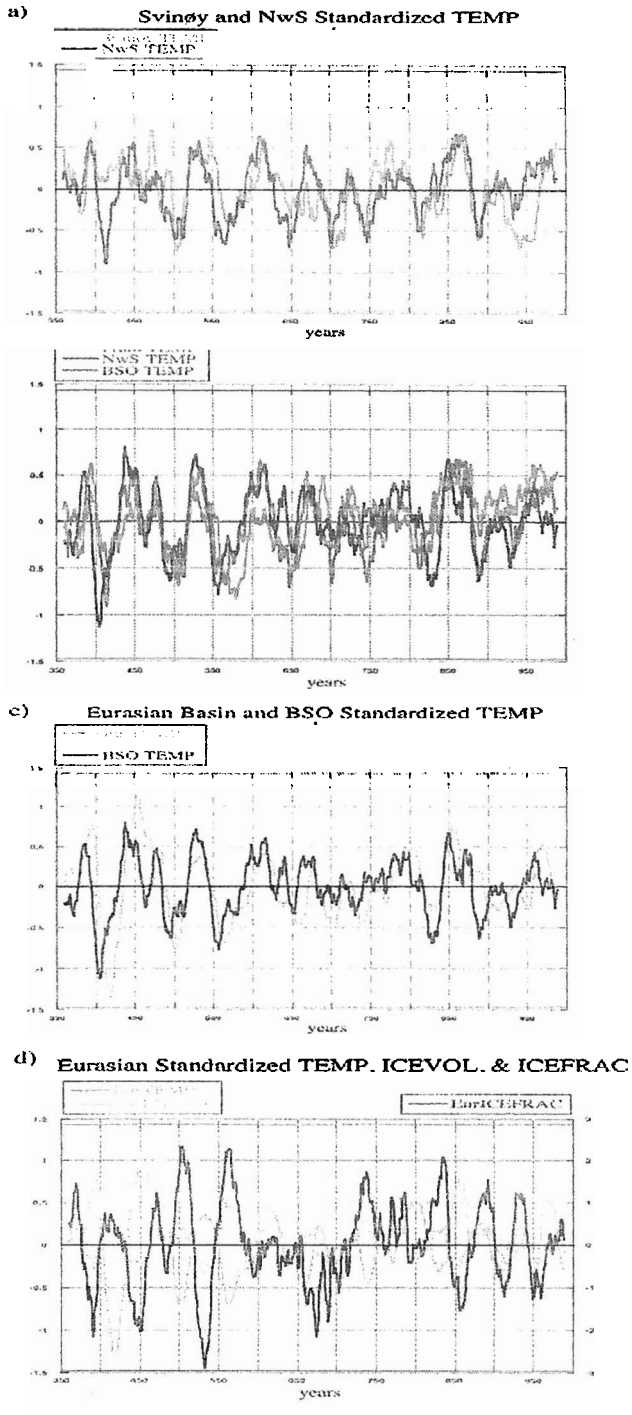

Figure 8. CCSM3 standardized transect and basin temperatures with 20-year smoothing for: a) the Svinøy and Norwegian Sea, b) the Fram Strait, Norwegian Sea, and BSO. c) the BSO and Eurasian Basin, and d) the Eurasian Basin temperature along with Eurasian ice volume and ice fraction.

20-year smoothing, the correlation analyses were done on the un-smoothed time series. Tracking the AW inflow northward to the Arctic Ocean, the Svinøy temperature time series is compared with the NwS temperature time series (Figure 8a). The two are correlated at r=0.50 (99%), with lag correlation analysis revealing that the Norwegian basin temperatures lag those seen through the Svinøy transect by 3 years. The NwS temperature time series is compared with AW inflow temperatures from the BSO and the Fram Strait (Figure 8b). The NwS and BSO temperature time series are significantly correlated, with r=0.60 (99%). However, the NwS and Fram Strait temperatures are only correlated at r=0.069 (92%), suggesting different processes occur in these two regions. Correlating the BSO time series with the Eurasian Basin temperatures (Figure 8c), the correlation coefficient is 0.52 (99%). Also, the Fram Strait temperature time series is correlated with the Eurasian Basin, and the two are significantly correlated with r=0.43 (99%). Through lag correlation analysis, it is found that temperatures in the Eurasian basin lag both the BSO and the Fram Strait temperature inflows by 4 years. The Eurasia and Canadian Basin temperatures were correlated with r=0.52 (99%), and lag correlation analysis revealed that the Canadian Basin temperatures lag those in the Eurasian Basin b 6 years. Therefore, it takes approximately 13 years for heat transport anomalies seen at the Svinøy transect to reach the Canadian Basin. This compare favorably with the observational propagation times of 9-15 years (Simonsen and Haugen 1996; Polyakov et al. 2004).

The Eurasian Basin temperature shows a significant negative correlation (Figure 8d) with both ice fraction, r=-0.284 (99%), and ice volume, r=-0.96 (99%); exhibiting decreased sea ice in the Eurasian Basin occurring in conjunction with warm Eurasian temperature anomalies. Results are presented for Eurasian Basin sea ice only, since Canadian Basin sea ice is less variable. All CCSM3 variables exhibit MDV, which can b analyzed further by compositing warm and cold periods.

e. Warm and Cold Composites in the CCSM3

Using a de-trended Eurasian Basin temperature time series with a 20-year smoothing, epochs were chosen as anomalies greater than 0.5 σ and which were sustained for more than 5 years. From these criteria, seven warm periods and nine cold periods (see Table 1), were identified and used for constructing warm and cold composites.

Warm and Cold Composites

Table 1. CCSM3 years extracted from the Eurasian Basin temperature time series as warm and cold epochs.

CCSM3 control run (b30.004)	WARM	COLD
YEARS	385-403	408-434
	449-487	494-513
	523-543	555-594
	611-627	651-669
	789-813	693-712
	846-867	735-749
	962-980	778-835
		909-917
		949-956

i. Composite Analysis

Epochs for volume flux, heat transport, AW inflow and basin temperatures, SHF, ice fraction, and ice volume, were constructed using the leads from the Eurasian Basin temperature time series discussed above in section d. ii. Composites for warm and cold periods were then created by averaging over time, see Figure 9, where warm (cold)

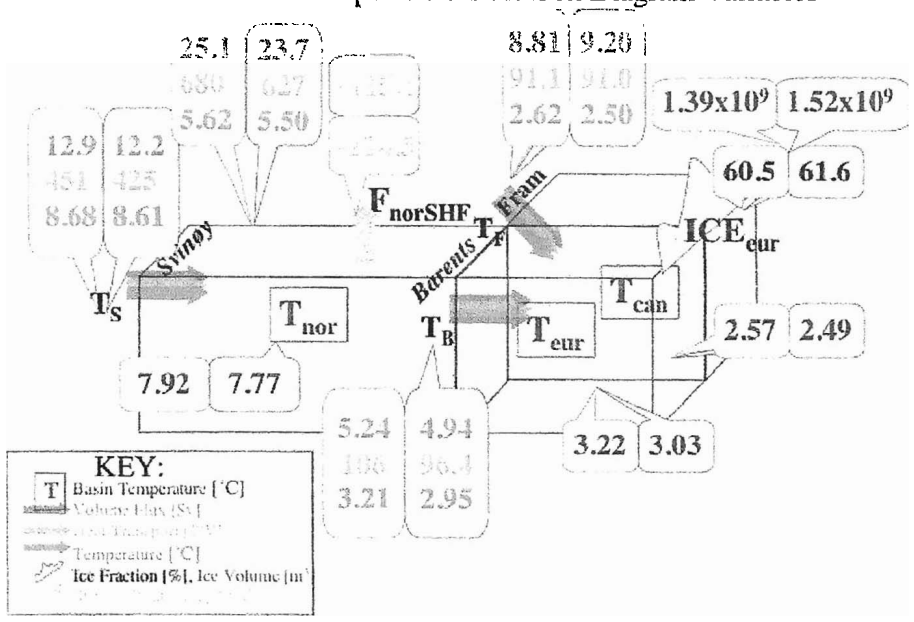

Figure 9. CCSM3 warm (red) and cold (blue) composites for the box diagram variables.

composites are outlined in red (blue).

Consistent differences were found between the warm and cold composites. Warm (cold) epochs are characterized by; increased (decreased) temperature, volume flux, and heat transport in the AW inflow regions, increased (decreased) ocean basin temperatures, and a decreased (increased) SHF with decreased (increased) ice fraction.

The exception to this occurs in the Fram, where during warm periods there is a slight decrease in volume flux yet a small increase in heat transport. This suggests that the incoming ocean temperature was anomalously warm, and the circulation is weak. In the cold composites for the Fram, there are slight increases in volume flux and heat transport. In this case, the incoming temperature is anomalously cold, but the circulation is stronger than normal. Hence, both warm and cold composites for the Fram Strait, result in a slight increase of heat transport, but for different reasons.

If the mean heat transport through the Fram and BSO is summed together (Figure 5), a combined heat transport of 192 TW is found going into the Arctic Ocean. Comparing the

warm and cold composites seen in Figure 9, a combined total of 197 TW from the Fram and BSO is going into the Arctic during warm periods, versus 187.5 TW during cold periods. This implies a difference of 10 TW between warm and cold epochs, with anomalies of about 5 TW. Now, assuming a heat transport increase of 1 TW, the heat (Q) added per year is 0.32×10^{22} Joules (see Appendix A). For the mass of the Arctic Ocean down to 1000 m, (80-90°N, 0-360° longitude), this calculates to a temperature change of 0.03 °C per year. For anomalies of 5 TW, this implies an Arctic Ocean basin temperature change of 0.15 °C per year. Using the difference between warm and cold composites, 10 TW is equivalent to a temperature change of 0.3 °C per year. This is comparable to what is seen in Figure 9, where the temperature difference between warm and cold composites for the Eurasian Basin is 0.019 °C, and for the Canadian Basin 0.08 °C.

ii. Ocean TEMP and Circulation

Changes in the ocean circulation of the North Atlantic can have a large effect on the volume and heat transports of AW into the Arctic; so next we examine the anomalous temperature and ocean circulation for the CCSM3 warm and cold composites. Figure 10a

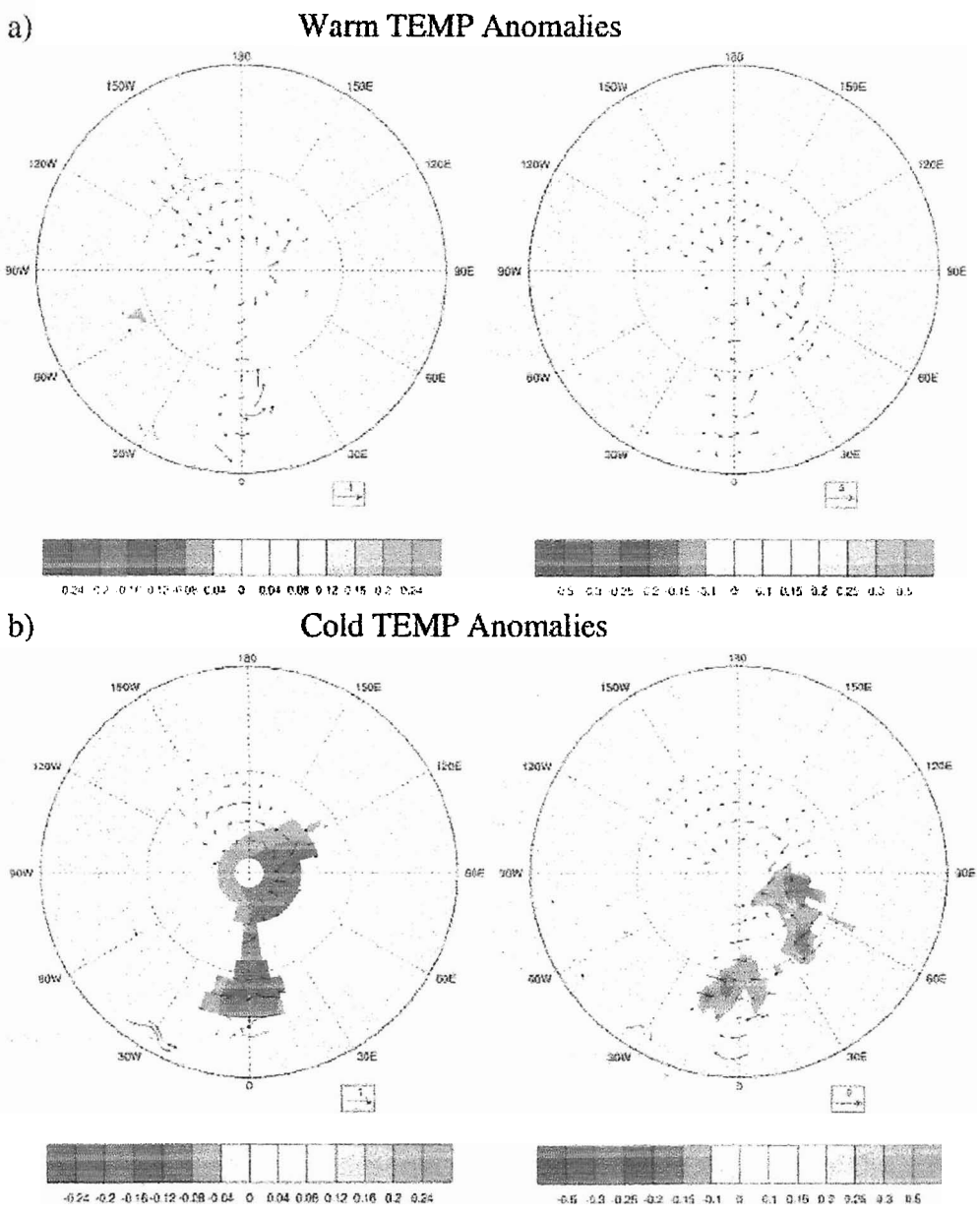

Figure 10. a) Warm composite anomalies for temperature [°C] and circulation vectors at the 317 m and 50 m layers with 0.1 [cm/s] and 0.5 [cm/s] reference vectors and b) similar cold composite anomalies.

(10b) shows warm (cold) composite anomalies of AW temperature along with zonal (U) and meridional (V) current vectors for the 317 m layer, as well as, ocean potential temperature and currents for the 50 m layer. The 317 m layer circulation is also a

representative depth for the AW layer circulation in the Arctic basin (recall Figure 2b), and the 50 m layer temperature and circulation better represents the AW layer inflow through the NwS and the Svinøy and BSO transects.

For the warm composites, positive temperature anomalies are seen throughout the Norwegian, Barents, and Kara Seas, with the anomalous maxima seen coming through the St. Anna Trough and into the Eurasian Basin. There is anomalously strong north/northeast circulation in the Norwegian Sea and AW subduction zone. This is consistent with the increased volume flux and heat transport seen through the Svinøy and BSO transects in Figure 9. There is also anomalous southward flow seen between Svalbard and Franz Josef Land. This, together with the increased northeasterly flux from the NwS and BSO, supports the idea of an increased boundary current quickly transferring heat through the border seas. This explanation also agrees with the location of the anomalous temperature maxima. North of 75°N on the prime meridian, the anomalous circulation vectors are directed west. This would imply a decreased AW inflow through the Fram during warm composites, which agrees with values taken from the warm/cold composites (Figure 9). Within the Arctic Ocean interior, there is anomalous cyclonic circulation, implying a weakening of the atmospheric polar high.

For the cold composites, negative temperature anomalies are seen throughout the AW inflow regions, with the anomalous maxima again found coming through the St. Anna Trough, but now also located between Iceland and Svalbard. There is anomalous westward flow seen throughout the Norwegian Sea, which likely contributes to the cold temperatures located between Iceland and Svalbard. In this region, north of 75°N, there are anomalous easterlies, which would allow for increased transport of the anomalously cold AW through the Fram Strait and into the Arctic. This is consistent with transport values from Figure 9. In the Barents Sea, there is anomalous northward transport between Svalbard and Franz Josef Land with anomalous westerlies seen along the coast in the region of easterly boundary currents. This implies a weakening of the Nordic Seas boundary current, but with an increased amount of AW flow found along the south

border of Franz Josef Land. There is also an increased anticyclonic circulation seen over the Arctic Basin interior.

Within the CCSM3 AW thermodynamic system, there appears to be a regulatory internal oceanic feedback mechanism that could help account for AW oscillations between warm and cold periods. In comparing AW heat transports into the Arctic between warm and cold composites, note that warm epochs are characterized by increased flow through the BSO, versus increased flow through the Fram during cold composites. Since the Fram Strait is the major inflow pathway for AW, this suggests that the anomalous south/southwesterly flow seen through the Fram during warm periods, actually acts to slow the amount of anomalously warm water allowed into the Arctic, and may also help to export more flow out of the Arctic as well. However, during cold periods, increased flow seen through the Fram acts to increase the amount of warm AW inflow transported into the Arctic. Thus, the anomalous ocean circulation found during warm/cold periods, acts as a negative feedback upon the AW thermodynamic system. The anomalous ocean circulation likely occurs as a result of internal ocean dynamics, as well as anomalous atmospheric temperature and SLP changes.

iii. SLP, Tref, and ICEFRAC

Due to the important role played by air-sea interaction in climate anomalies of the North Atlantic sector, the atmosphere must also be considered in the context of multi-decadal variability. Figure 11 displays the CCSM3 climatological mean along with warm and cold composite anomalies for the atmospheric a) Reference Height Temperature (TREFHT, or T_{ref}), b) Sea Level Pressure (SLP), and c) ice fraction.

a) MEAN, WARM - MEAN, and COLD - MEAN for TREFHGT [°C]

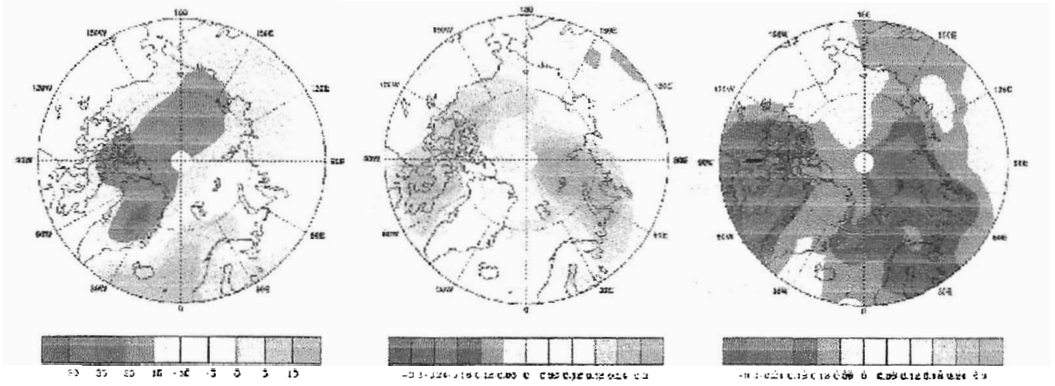

b) MEAN, WARM - MEAN, and COLD - MEAN for PSL [hPa]

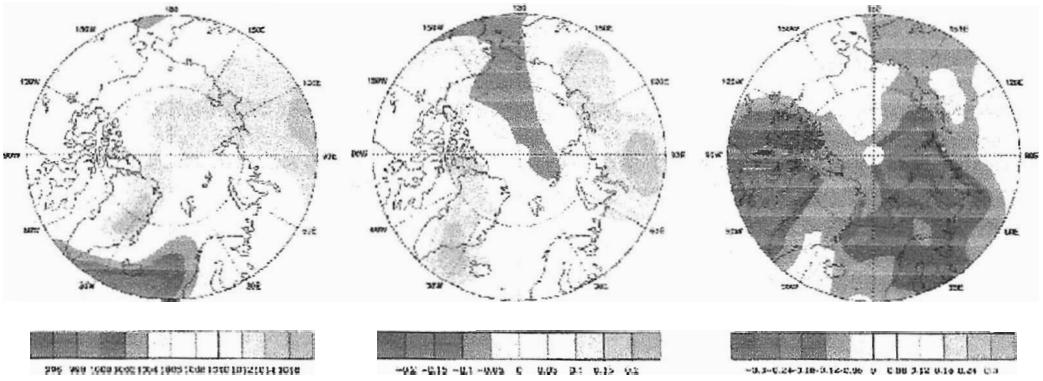

c) MEAN, WARM - MEAN, and COLD - MEAN for ICEFRAC [%]

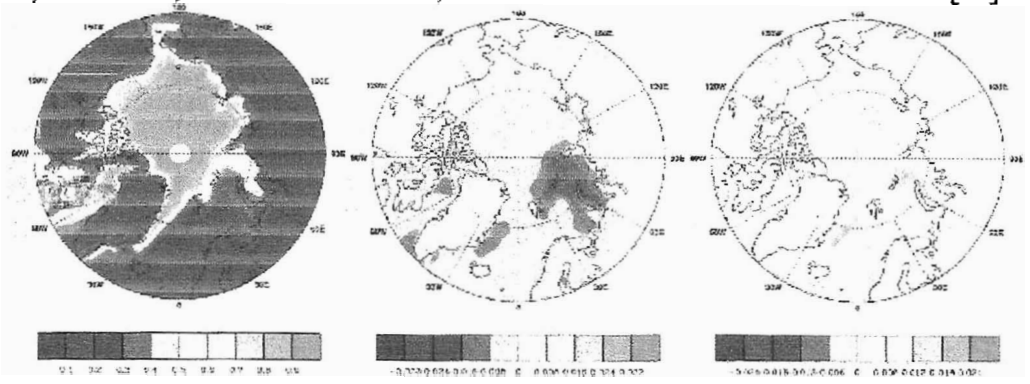

Figure 11. (L to R) Climatology, along with warm and cold composite anomalies for a) TREFHT [°C], b) SLP [hPa], and c) ICEFRAC [%].

During the warm periods, strong positive T_{ref} anomalies are found over the Kara Sea, northward between Franz Josef Land and Severnaya Zemlya, and continuing on north to the pole (Figure 10a, center plot). This agrees well with the location of anomalous ocean temperature extrema found in Figure 10a. Positive T_{ref} anomalies are also seen spanning across the Canadian Archipelago into the Beaufort Sea. SLP composites (Figure 11b) show a decrease in the climatological high-pressure system located over the central Arctic Ocean, with an increase in the high-pressure systems located over Greenland and the northern Eurasian continent. Also, the climatological low-pressure system found spanning across the North Atlantic to Norway is weakened. The result is two strong segmented highs located over Greenland and northern Eurasia, with a weakened low-pressure system across the North Atlantic and a weakened polar high found in the interior. The strengthened high located over northern Eurasia is consistent with ocean temperature and circulation anomalies found in Figure 10a, allowing for the increased northeasterly flow through the BSO and an accelerated boundary current. The weakened polar high also agrees with the anomalous southward flow found between Svalbard and Franz Josef Land as well as the anomalous cyclonic circulation seen in the Arctic interior (Figure 10a). Decreased amounts of ice fraction (Figure 11c) can be seen in the Kara Sea, and between Franz Josef and Severnaya Zemlya, consistant with the spatial extent of positive atmospheric and oceanic temperature anomalies (Figures 11a & 10a).

During the cold periods, strong negative T_{ref} anomalies are again found over the Kara Sea, northward between Franz Josef Land and Severnaya Zemlya, and extending towards the pole and to the Canadian Archipelago (Figure 11a). The below normal T_{ref} anomalies over the Kara Sea and Eurasian Basin are co-located with anomalously cool ocean temperatures (Figure 10b). The cold composites of anomalous SLP (Figure 11b), show a strong polar high located over the interior Arctic Ocean with the maximum anomaly extending northward between Franz Josef Land and Severnaya Zemlya. The strong polar vortex is consistent with the increased anti-cyclonic ocean circulation seen in the Arctic interior (Figure 10b), as well as with anomalously cool T_{ref} and ocean temperature. The climatological high-pressure system located over Greenland is weakened, and there is a

strong low-pressure system extending from approximately 60°N to 75°N, from the coast of Norway to 60°E. This low-pressure anomaly is essential in creating the anomalous westward flow seen the Norwegian and Barents Seas (Figure 10b). Positive ice fraction anomalies (Figure 11c) are found off the east coast of Greenland, extending from Iceland to Svalbard. This increase in ice fraction seen during the cold periods is likely the result of: 1) negative ocean and air temperature anomalies, 2) anomalous westerly flow south of Svalbard, and 3) build-up from converging ice export out of the Fram Strait.

IV. Summary and Conclusions

A multi-century coupled CCSM3 control simulation was used to examine the MDV of AW of the Arctic. The AW core temperature (AWcoreTEMP), ranges from 2-3 °C (Figure 2a), which is warmer than observations by 1-1.5 °C. The depth range of the AW core (AWcoreDEPTH) compares favorably with observations, ranging between 150-500 m. The CCSM3 was found to be capable of reproducing some of the key observed features of the AW circulation in the Arctic Basin interior, however, the boundary currents in the Nordic Seas are weak and the AW inflow circulation through the Fram Strait slightly underestimated.

Warm and cold periods are evident in area averaged[5] time series of the AWcoreTEMP and AWcoreDEPTH (Figure 7). Warm (cold) AWcoreTEMPs occur along with shallow (deep) AWcoreDEPTHs, with a thickening (thinning) in the AW layer seen during warm (cold) periods. This is in agreement with observations of increased AW volume and heat transports, along with shoaling of the AW core, occurring during warmer periods (Polyakov et al. 2004).

Volume flux, heat transport, and inflow temperature from the: Svinøy Transect [63°N, 3°E], Fram Strait [79.5°N, 3-8.5°E], and BSO [71-79.5°N, 31°E], were compared with data from observational mooring transects for validation of model circulation. Although the temperature in the model is generally warmer than the observational data, the

[5] [80-90°N, 0-360°E]

temperature versus depth profiles (Figure 4) reveal that CCSM3 realistically captures the vertical extent and temperature characteristics of the AW layer in the inflow regions to the Arctic. Hence, the CCSM3 is a valuable tool for investigating mechanisms of multi-decadal variations in oceanic volume and heat fluxes to the Arctic.

The model circulation (Figure 5) generally displays stronger volume fluxes than observed, except in the Fram Strait where there is a weaker than observed volume flux. This, together with the generally warmer temperatures, results in model heat transports that are higher than what is found in nature. The variability (σ_{5yr}'s) found in the CCSM3 for volume flux, heat transport, and temperature, was well within the range of observed variability.

Along with the volume flux, heat transport, and temperature data taken from AW inflow transects (Figure 5) climatological means for the CCSM3 variables of SHF, ocean basin temperature, ice fraction, and ice volume, were also analyzed (Figure 6). Time series (Figure 8) for the CCSM3 variables depicted in Figures 5 and 6 were correlated to determine coherence between the AW transport variables, as well as, estimate the time taken for heat anomalies to propagate from the Svinøy transect to the Arctic interior. All box diagram variables (Figure 3) were significantly correlated, with lag correlation analysis revealing that it takes approximately 13 years for heat transport anomalies seen at the Svinøy transect to reach the Canadian Basin. This compares favorably with observed propagation times of 9-15 years for AW temperature anomalies to go from the AW subduction zones to the Arctic interior. Ice fraction and ice volume for the Eurasian Basin were also found to have a significant negative correlation with Eurasian Basin temperatures, thus, implying that warm (cold) AW temperatures in the Eurasian Basin occur in conjunction with decreased (increased) ice fraction and volume. All time series exhibited MDV, which was analyzed further by compositing warm and cold periods (defined in Table 1).

Warm (cold) composites were characterized by; increased (decreased) temperature, volume, and heat transports in the AW inflow transects, increased (decreased) ocean basin temperatures, and a decreased (increased) SHF with decreased (increased) ice

fraction. The exception to this occurs in the Fram, where increased (decreased) flow is seen during cold (warm) periods, resulting in slight increases of heat transport found during both warm and cold composites. If the heat transports for the Fram and BSO are added together, a difference of 10 TW of heat transported into the Arctic is found between warm and cold composites. This is equivalent to a temperature change of 0.3 °C per year, and the CCSM3 displays a combined Eurasian and Canadian Basin temperature difference of 0.27 °C (Figure 9).

Spatial composites for ocean temperature and circulation anomalies (Figure 10), reveal that during the warm (cold) periods, positive (negative) temperature anomalies could be seen throughout the Norwegian, Barents, and Kara Seas. Anomalous circulation composites suggest a weakening (strengthening) of the Arctic Ocean interior anti-cyclonic gyre during warm (cold) periods. Warm (cold) composites for ocean circulation anomalies located in the Barents Sea display; anomalous southward (northward) transport between Svalbard and Franz Josef Land, with anomalous easterlies (westerlies) seen along the coast. Also, AW inflow through the Fram Strait is decreased (enhanced) during warm (cold) periods.

Composites for the atmospheric variables reveal warm (cold) T_{ref} anomalies (Figure 11a) over the Kara Sea and Eurasian Basin are co-located with positive (negative) ocean temperature anomalies (Figure 9a,b). SLP composites (Figure 11b) show a decrease (increase) of the climatological high-pressure system located over the central Arctic Ocean during warm (cold) epochs, with the anomalous SLP tendency flow being consistent with anomalous ocean circulation vectors. During warm periods, decreased ice fraction anomalies can also be seen over the Kara Sea, with increased ice fraction anomalies occurring off the coast of Greenland during cold periods (Figure 11c).

An intriguing finding of this study was the existence of an internal ocean feedback mechanism that helps to regulate the oscillations of AW between warm and cold periods. When comparing AW heat transports between warm and cold composites, it was found that cold (warm) composites depict anomalously strong (weak) inflow through the Fram Strait, and vice versa for the BSO. Since the Fram Strait is the major inflow pathway for

AW, this suggests that the anomalous south/southwesterly ocean circulation seen through the Fram during warm periods, acts to slow the amount of anomalously warm water allowed into the Arctic. During cold periods, increased flow through the Fram acts to increase the amount of warm AW inflow transported into the Arctic. Hence, the anomalous ocean circulation found during warm/cold periods is a negative feedback upon the AW thermodynamic system. This regulatory ocean feedback mechanism likely occurs as a mixture of internal ocean dynamics, as well as anomalous atmospheric temperature and SLP changes.

V. Appendix A

The following equations were used to calculate volume flux and heat transport for the AW inflow transects.

$$\text{volume flux} = \iint U\,dx\,dz,\ \iint V\,dy\,dz, \quad [m^3 s^{-1}], \tag{1}$$

$$\text{heat transport} = rc_p \iint (T - T_{ref})U\,dx\,dz,\ rc_p \iint (T - T_{ref})V\,dy\,dz, \quad [Js^{-1} \equiv W], \tag{2}$$

where U & V are the zonal & meridional current vectors $[ms^{-1}]$, taken through the longitudinal/latitudinal cross – sectional area $[m^2]$, ocean density is $r \cong 1000\ [kgm^{-3}]$, specific heat is $c_p \cong 4000\ [Jkg^{-1}°C^{-1}]$, and T [°C], is the vertically averaged mean temperature, with $T_{ref} = 0.01$ [°C] (note: $1x10^6\ m^3s^{-1} = 1$ Sv, and $1x10^{12}$ W = 1 TW).

To determine how changes in heat transport would affect Arctic Ocean temperatures, the conservation of heat equation was used. Assuming a closed system,

$$Q = c_p m \Delta T, \tag{3}$$

where Q = heat added [J], specific heat is $c_p \cong 4000\ [Jkg^{-1}°C^{-1}]$,
m = mass [kg], and ΔT = change in temperature [°C].

Q, was taken as the difference in heat transport between warm and cold composites, with heat transport into the Arctic Ocean defined as the combined Fram Strait and BSO AW inflow transports. To calculate the Arctic Ocean temperature change, first, a 1 TW heat transport increment was used, and then followed by the difference in heat transport seen between warm and cold composites, 10 TW.

$$Q = 1\,\mathrm{TW} = 1\mathrm{x}10^{14}\,\mathrm{Js}^{-1} = 0.32\mathrm{x}10^{22}\,\mathrm{Jyr}^{-1}$$

$$V_{\mathrm{Arctic}} = 2.66\mathrm{x}10^{16}\,\mathrm{m}^3$$

$$m = rV = 2.66\mathrm{x}10^{19}\,\mathrm{kg}$$

$$Q = c_p m \Delta T$$

$$\Rightarrow \Delta T = \frac{1\,\mathrm{TW}}{(3994\mathrm{Jkg}^{-1}{}^{\circ}\mathrm{C}^{-1})(2.66\mathrm{x}10^{19}\,\mathrm{kg})}$$

$$\Rightarrow \Delta T = 0.03\,{}^{\circ}\mathrm{C}^{-1}\mathrm{yr}^{-1}$$

for $Q = 10$ TW,

$$\Rightarrow \Delta T = 0.3\,{}^{\circ}\mathrm{C}^{-1}\mathrm{yr}^{-1}$$

VI. Bibliography

Bengtsson, L., V. A. Semenov, and O. M.Johannessen, 2004: The Early Twentieth-Century Warming in the Arctic - A Possible Mechanism, J. of Clim., 17, 4045-4057.

Blackmon, M. B., et al.,: 2001: The Community Climate System Model. *BAMS*, **82**, 11, 2357-2376.

Briegleb, B. P., C. M. Bitz, E. C. Hunke, W. H. Lipscomb, M. M. Holland, J. L. Schramm, and R. E. Moritz, 2004: Scientific description of the sea ice component in the Community Climate System Model, Version Three. Tech. Note NCAT/TN-463+STR, National Center for Atmospheric Research, Boulder, CO, 70 pp.

Collins, W. D., C. M. Bitz, M. L. Blackmon, G. B . Bonan, C. S. Bretherton, J. A. Carton, P. Chang, S. C. Doney, J. J. Hack, T. B. Henderson, J. T. Kiehl, W. G. Large, D. S. McKenna, B. D. Santer, and R. D. Smith. The Community Climate System Model: CCSM3. *J. Climate*, in press.

Collins, W.D., P. J. Rasch, B. A. Boville, J. J. Hack, J. R. McCaa, D. L. Williamson, B. P. Briegleb, C. M. Bitz, S.-J. Lin, and M. Zhang. The Formulation and Atmospheric Simulation of the Community Atmosphere Model: CAM3. *J. Climate*, in press.

Collins, W. D., M. Blackmon, C. Bitz, G. B. Bonan, C. S. Bretherton, J. A. Carton, P. Chang, S. Doney, J. J. Hack, J. T. Kiehl, T. Henderson, W. G. Large, D. McKenna, B. D. Santer, and R. Smith, 2005: The Community Climate System Model: CCSM3. *J. Climate*, in press.

Danabasoglu, G.,W. G. Large, J. J. Tribbia, P. R. Gent, B. P. Briegleb, and J. C. McWilliams, 2005: Diurnal ocean-atmosphere coupling. *J. Climate*, in press.

Delworth, T. L., and M. E. Mann, Observed and simulated multi-decadal variability in the Northern Hemisphere, *Climate Dynamics*, **16**, 661–676, 2000.

Deser, Clara, John Walsh and Michael S. Timlin, 2000: Arctic Sea Ice Variability in the Context of Recent Atmospheric Circulation Trends, *J. Clim.*, **13**, 617-633.

Dickinson, R.E., K. W. Oleson, G. B. Bonan, F. Hoffman, P. Thornton, M. Vertenstein, Z.-L. Yang, X. Zeng. The Community Land Model and Its Climate Statistics as a Component of the Community Climate System Model, *J. Climate*, in press.

Enfield, D.B., A.M. Mestas-Nunez, and P.J. Trimble, 2001: The Atlantic Multidecadal Oscillation and its Relation to Rainfall and River Flows in the Continental U.S., *Geos. Res. Lett.*, **28**, 10, 2077-2080.

Mork, Kjell Arne and Johan Blindheim, 2000: Variations in the Atlantic inflow to the Nordic seas, 1955-1996. *Deep-Sea Research I*, **47**, 1035-1057.

Oleson, K. W., Y. Dai, and Coauthors, 2004: Technical description of the Community Land Model (CLM). NCAR Tech. Note TN-461+STR, 174 pp.

Orvik, Kjell Arild and Oystein Skagseth, 2005: Heat flux variations in the eastern Norwegian Atlantic Current toward the Arctic from moored instruments, 1995-2005, *Geos. Res. Lett.*, **32**, L14610.

Orvik, Kjell Arild, Oystein Skagseth, and Martin Mork, 2001: Atlantic Inflow to the Norwegian Seas current structure and volume fluxes from moored current meters, VM-ADCP and SeaSoar-CTD observations, 1995-1999, *Deep-Sea Research I*, **48**, 937-957.

Polyakov, I. V., G. V. Alekseev, L.A.Timokhov, et al., 2004:Variability of the Intermediate Atlantic Water of the Arctic Ocean over the Last 100 years, *J. of Clim.*,**17**, 23, 4485-4497.

Polyakov, I. V., G. V. Alekseev, R. V. Bekryaev, et al., 2002b: Observationally based assessment of polar amplification of global warming, *Geos. Res. Lett.*, **29**, 18, 251-254.

Polyakov, Igor V. and Mark Johnson, 2000: Arctic decadal and interdecadal variability, *Geos. Res. Lett.*, **27**, 24, 4097-4100.

Schauer et al. 2004: Arctic Warming through the Fram Strait: Oceanic heat transport from 3 years of measurements. *J. of Geophys. Res.*, **109**, C06026.

Schlesinger, M.E., and N. Ramankutty, 1994: An Oscillation in the Global Climate System of Period 65-70 Years. *Nature*, **367**, 723-726.

Simonsen, Knud, and Peter M. Haugen, 1996: Heat Budgets of the Arctic Mediterranean and sea surface heat flux parameterizations for the Nordic Seas. *J. of Geophys. Res.*, **101** C3, 6553-6576.

Smith, R. D. and P. R. Gent, 2002: Reference manual for the Parallel Ocean Program (POP), ocean component of the Community Climate System Model (CCSM2.0 and 3.0) Technical Report LA-UR-02-2484, Los Alamos National Laboratory, available online a http://www.ccsm.ucar.edu/models/ccsm3.0/pop.